Geobiology

WILEY

gebiology

ORIGINAL ARTICLE

Thallium Isotopes Suggest the Global Deep Ocean Did Not Approach Modern Oxygenation During Cambrian Age 3 Metazoan Radiation

Jean N. R. Clemente[1,2] | Haifeng Fan[3,4] | Chadlin M. Ostrander[5] | Hongjie Zhang[3,4] | Hanjie Wen[4,6] | Erik A. Sperling[7] | Sune G. Nielsen[2,8]

[1]MIT-WHOI Joint Program in Oceanography, Woods Hole, Massachusetts, USA | [2]Department of Geology and Geophysics, Woods Hole Oceanographic Institution, Woods Hole, Massachusetts, USA | [3]State Key Lab of Ore Deposit Geochemistry, Institute of Geochemistry, CAS, Guiyang, China | [4]University of Chinese Academy of Sciences, Beijing, China | [5]Department of Geology & Geophysics, University of Utah, Salt Lake City, Utah, USA | [6]School of Earth Sciences and Resources, Chang'an University, Xi'an, China | [7]Department of Earth and Planetary Sciences, Stanford University, Stanford, California, USA | [8]CRPG, CNRS, Université de Lorraine, Nancy, France

Correspondence: Jean N. R. Clemente (jeanrc2@mit.edu) | Haifeng Fan (fanhaifeng@mail.gyig.ac.cn)

Received: 16 October 2024 | **Revised:** 10 July 2025 | **Accepted:** 28 July 2025

Funding: This work was supported by National Natural Science Foundation of China (Grants 42121003 and 41890841), Guizhou Provincial Science and Technology Department (Grant GZ2020SIG), National Aeronautics and Space Administration (Grant 80NSSC24K0845) and National Science Foundation (Grant EAR-2143164).

Keywords: Cambrian explosion | ocean oxygenation | paleoredox | thallium isotopes

ABSTRACT

The geologically rapid appearance of most extant animal groups in the Cambrian fossil record is often linked to enhanced ocean oxygenation. However, conflicting reconstructions of the Cambrian redox landscape make it difficult to determine the extent of ocean oxygenation during this significant biotic event, particularly regarding the redox state of the global deep ocean. In this study, we present authigenic thallium isotope compositions ($\varepsilon^{205}Tl_{auth}$) for two shale sequences from South China (Qingjiang and Weng'an) that span the Cambrian Stage 2–3 boundary to the appearance of the Qingjiang biota, approximately 521–518 million years ago (Ma), a timeframe that chronicles a particularly rapid interval of metazoan diversification and radiation in the broader Cambrian explosion. If this event occurred amid modern-like extents of global ocean oxygenation, we would expect a significant increase in the global extent of seafloor Mn-oxide burial to drive lower $\varepsilon^{205}Tl_{auth}$ values near the modern open-ocean composition of −6‰. Instead, we observe broadly stable $\varepsilon^{205}Tl_{auth}$ values of around −3 to −4‰ in both studied sections. The lack of any significant Tl isotope shifts in our dataset argues against a short-term global ocean oxygenation event and suggests the global deep ocean was not characterized by modern extents of oxygenation 521–518 Ma. We reinterpret contemporaneous near-modern Mo and U isotope compositions to signal a relatively minor increase in marine oxygenation, likely limited to the continental shelves. However, $\varepsilon^{205}Tl_{auth}$ lower than the average isotopic composition of approximately −2‰ in Ediacaran shales suggests a shift to comparatively better-oxygenated conditions sometime between ~555 Ma and 521 Ma. If diversification at this time was linked to increased ocean oxygen levels, these changes were likely more dominant in the relatively shallow-water settings of continental shelves most densely populated by Cambrian animals and were incapable of dramatically altering seawater Tl isotope mass balance through seafloor Mn-oxide burial.

1 | Introduction

The rapid radiation of most extant animal groups in the early Cambrian approximately 540–520 million years ago (Ma) marks the pivotal biotic event dubbed the Cambrian explosion (Knoll and Carroll 1999; Marshall 2006). Fossil evidence that metazoans were unambiguously present ~40 My prior—as well as organic biomarker and molecular clock evidence they were possibly present as far back as the Tonian or Cryogenian (Dohrmann and Wörheide 2017; Knoll and Carroll 1999; Love et al. 2009)—has led multiple studies to interpret the Cambrian explosion in the context of changing environmental conditions that abruptly permitted, or promoted, metazoan radiation (e.g., Knoll and Carroll 1999; Wood et al. 2019). However, the search for a principal environmental trigger for the Cambrian explosion remains elusive.

One hypothesis that has garnered continued interest is the role of changing molecular oxygen (O_2) availability in seawater. The free energy yield from aerobic respiration is significantly greater than that of other oxidants, offering a plausible energy source for some ecological innovations that first appear in the Cambrian fossil record (e.g., Payne et al. 2009). Similar changes in body plan and ecological complexity found today along oxygen gradients in marine Oxygen Minimum Zones (OMZs) offer a tentative analog to the coupled changes in marine redox and metazoan diversity during the Cambrian (Rhoads and Morse 1971; Sperling et al. 2013). To this point, a shift in the scale of global seafloor oxygenation has long been hypothesized as a trigger for early animal radiation.

Many recent geochemical studies infer intervals of greater marine oxygenation during the early Cambrian (Chen et al. 2015; Cheng et al. 2017; Fan et al. 2023; Feng et al. 2014; Jin et al. 2016; Li et al. 2017, 2021; Wei et al. 2020; Wen et al. 2015). However, the validity and scale of these oxygenation events, chiefly the extent of deep marine oxygenation, remain a subject of intense debate. The discovery of a few sedimentary U and Mo isotope compositions comparable to today has led to a straightforward interpretation that oceans were characterized by a near-modern redox state (i.e., with large extents of moderately or strongly oxic regions) near the Cambrian Age 2–3 boundary (~521 Ma), coeval with an exponential increase in global metazoan diversity (Chen et al. 2015; Dahl et al. 2017; Li et al. 2021; Wen et al. 2015). In this framework, a substantial global oxygenation event could have facilitated diversification by expanding habitable settings and removing limitations to the O_2 demands of Cambrian body plans (Chen et al. 2015). However, other geochemical datasets, including changes in Fe species ratios, redox-sensitive element (RSE) concentrations, and other Mo and U isotope datasets, seem to indicate that the global deep ocean remained broadly anoxic in the early Cambrian with strongly heterogeneous marine redox conditions (Cheng et al. 2017; Feng et al. 2014; Jin et al. 2016; Qin et al. 2022; Sperling, Knoll, and Girguis 2015; Stockey et al. 2024; Wei et al. 2018, 2021). Metazoan diversification under this framework may have been triggered by more subtle but still ecologically important changes to ocean oxygenation or other environmental/ecological factors in the shelf environments most densely inhabited by Cambrian animals. Evidently, additional research is required to address the ongoing debate surrounding the redox evolution of Cambrian oceans.

Stable thallium (Tl) isotopes offer a novel approach to indirectly track changes in deep ocean oxygenation through Tl adsorption onto Mn(III/IV)-bearing oxides on the deep seafloor (e.g., Ostrander et al. 2017; Them et al. 2018). Differences in the ratio of the two stable Tl isotopes, ^{203}Tl and ^{205}Tl, are expressed relative to the NIST 997 Tl standard:

$$\varepsilon^{205}\mathrm{Tl}(‰) = \left(\frac{^{205/203}\mathrm{Tl}_{\mathrm{sample}}}{^{205/203}\mathrm{Tl}_{\mathrm{NIST-997}}} - 1 \right) \times 10^4$$

In the modern ocean, scavenging of Tl(I) and its subsequent oxidation to Tl(III) by Mn oxides imparts a strong positive isotope fractionation effect that enriches the oxides in ^{205}Tl (Nielsen et al. 2013; Peacock and Moon 2012; Rehkämper et al. 2002). This fractionation effect is mineral-specific and is most positive in Mn oxides that precipitate in cold, well-oxygenated seawater on the deep seafloor, as opposed to those of diagenetic or hydrothermally sourced Mn oxides (Peacock and Moon 2012; Phillips et al. 2023). Today, the deep ocean is broadly oxygenated such that extensive seafloor Mn oxide burial (and consequently ^{205}Tl scavenging) yields an open ocean isotopic composition that is notably lower than global ocean inputs ($\varepsilon^{205}Tl_{seawater} = -6.0‰$ compared to $\varepsilon^{205}Tl_{in} \approx -2‰$; Owens et al. 2017; Rehkämper et al. 2002; Wang et al. 2022). Because the ~20 ky marine residence time of Tl is longer than the ocean mixing time of ~1 ky, $\varepsilon^{205}Tl_{seawater}$ today is globally homogenous in the open ocean and sensitive to short-term changes in marine redox at least within a few thousand years (Rehkämper and Nielsen 2004). By contrast, in sediments with reducing porewaters near the sediment–water interface or beneath an anoxic water column, Tl is buried, likely with sulfides (Owens et al. 2017), with no resolvable fractionation effect. Sediments deposited under such reducing conditions record the contemporaneous $\varepsilon^{205}Tl_{seawater}$ value (e.g., Fan et al. 2020; Owens et al. 2017; Wang et al. 2022).

By extension, sedimentary sulfides from ancient sediments inferred to have been deposited under reducing waters with sufficient water-mass exchange with the open ocean can be used to reconstruct the $\varepsilon^{205}Tl_{seawater}$ of the contemporaneous water column (Nielsen et al. 2011; Owens et al. 2017). Analogous to today, sulfide-bound "authigenic" $\varepsilon^{205}Tl$ can be used to infer past changes in global Mn oxide burial on the deep seafloor. A broadly anoxic ocean would be expected to carry $\varepsilon^{205}Tl_{seawater}$ values near the isotopic value for global inputs ($\varepsilon^{205}Tl \approx -2‰$, similar to continental crust; Nielsen et al. 2005). Alternatively, if the Age 2–3 diversification event occurred in conjunction with a global marine oxygenation event to near-modern extents as has previously been suggested (Chen et al. 2015), we would expect a shift toward more negative, possibly near-modern, values (i.e., −6‰).

In this study, we address the conflicting paleoredox interpretations of the early Cambrian and present authigenic $\varepsilon^{205}Tl$ records for two black shale sequences from the Nanhua Basin, South China, that span the upper part of Cambrian Stage 2 to the lower part of Stage 3 from ~521 to 518 Ma. We test whether the Tl isotope composition of these shales approaches modern values of −6‰, which would be expected in an ocean with modern extents of oxygenation. We investigated Cambrian redox variability in two sections inferred

to have been deposited along the shelf proximal to a deep ocean basin: the Qingjiang core from Yichang, deposited in a shallow shelf environment, and outcrops of the Niutitang Formation at Weng'an, deposited in a deeper, more distal shelf environment. The Shuijingtuo Formation represented in the Yichang drill core contains the exceptionally preserved Qingjiang biota, and analyses of $\varepsilon^{205}Tl_{auth}$ trends relative to Age 2–3 diversification are made in the context of their appearance at ~518 Ma (Fu et al. 2019). Globally, the Age 2–3 interval represents a dramatic increase in the number of animal body plans (as recorded by first appearances of Linnean phyla and classes; Erwin et al. 2011). References to the "Cambrian explosion" in this study refer to this exponential increase in body plan disparity recorded in the fossil record, although it is recognized that early animal evolution was a protracted event (Wood et al. 2019).

2 | Materials and Methods

2.1 | Study Sections

In the late Neoproterozoic, intermittent phases of rifting between the Yangtze and Cathaysian blocks that comprised the South China craton formed the NE-trending intracontinental Nanhua Basin (Wang and Li 2003). Previously published stratigraphic frameworks for the basin recognize a broad transition from shallow-water carbonates in the northwest Yangtze Platform to deep-water shales and cherts in the southeast in strata deposited in the upper Ediacaran to lower Cambrian (e.g., Jin et al. 2016; Wang and Li 2003). This study focuses on the Qingjiang and Weng'an sections near the slope/basin transition (Figure 1).

Stratigraphy of the Qingjiang and Weng'an sections was previously described by Fan et al. (2023) and Jin et al. (2016), respectively, and was used to correlate three stratigraphic intervals (I-III) recognized in several South China sequences (Figure 1). The Interval I-II boundary is marked by a widespread Ni-Mo layer in both sections that has been dated to ~521 ± 5 Ma (Jin et al. 2016; Xu et al. 2012) in both the Qingjiang (lower Shuijingtuo Formation) and Weng'an (lower Niutitang Formation) sections. The beginning of Interval III is marked by the appearance of the Qingjiang biota in the Qingjiang section and a coeval lithological shift to mudstones in the Weng'an section. This boundary has been correlated with the ~518 Ma appearance of the Chengjiang biota in a less distal outer shelf setting than that of the Qingjiang biota (Fu et al. 2019; Han et al. 2018; Jin et al. 2016; Yang et al. 2018). Assuming sedimentation rates at each location were constant over time, age models were calculated using a linear extrapolation of these two stratigraphic markers primarily to facilitate data comparison between the Weng'an and Qingjiang sections.

2.2 | Element Concentrations and Fe-Speciation

Trace element (Mo, U, Tl) and major element (Fe, Al) concentrations of Qingjiang samples were measured using an inductively coupled plasma mass spectrometer (ICP-MS) at the ALS

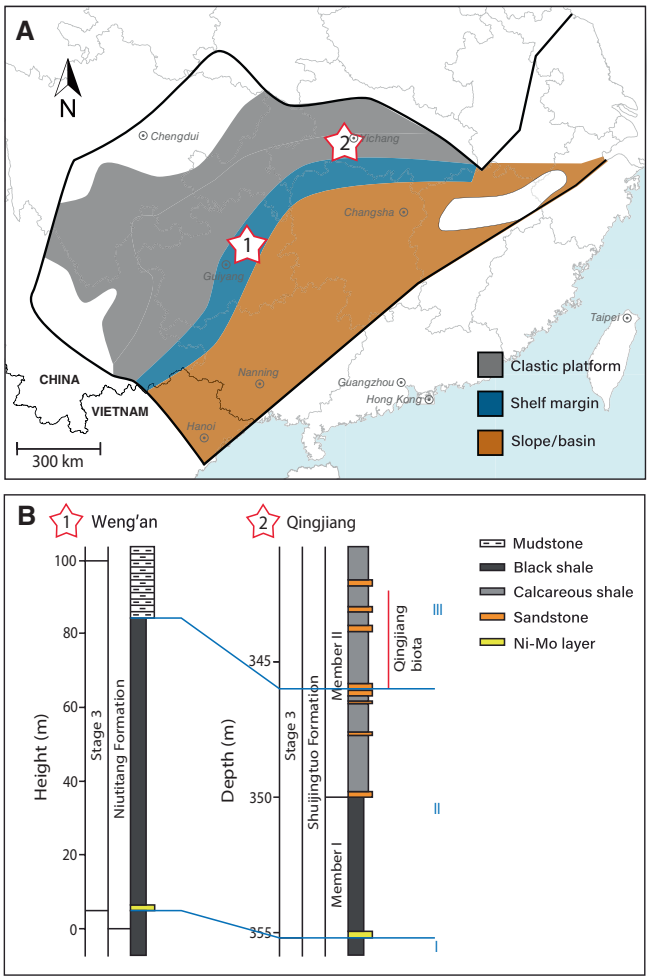

FIGURE 1 | (A) Paleogeographic map of the Nanhua Basin in South China, delimiting the shelf/platform and slope/basin depositional facies belts (modified from Chen et al. (2015)). The locations of the Weng'an outcrop (1) and Qingjiang core (2) are highlighted. (B) Stratigraphic correlation of the two sections. Stratigraphic descriptions are adapted from Fan et al. (2023) and Han et al. (2018).

Chemex facility in Guangzhou, China, following a four-acid (HCl-HNO_3-HF-$HClO_4$) digestion. The relative standard deviations (RSD) for these elements were less than ±10%. Trace element concentrations are expressed as enrichment factors (Mo_{EF} and U_{EF}), where total metal concentrations are normalized to sample Al and compared to the metal/Al of the bulk continental crust ($X_{EF} = [X]/[Al]_{sample}/[X]/[Al]_{crust}$; Rudnick and Gao 2014).

Iron species are composed of highly reactive Fe (Fe_{HR}) and residual Fe (Fe_R), which were measured at Chengdu Science and Technology University. Highly reactive Fe includes carbonate-associated Fe (Fe_{carb}), ferric oxides (Fe_{ox}), magnetite (Fe_{mag}), and pyrite (Fe_{py}) (i.e., $Fe_{HR} = Fe_{carb} + Fe_{ox} + Fe_{mag} + Fe_{py}$). Fe_{carb}, Fe_{ox}, and Fe_{mag} were sequentially extracted by a sodium acetate solution, a sodium dithionite solution, and an ammonium oxalate solution following methods from Poulton and Canfield (2005) and Li et al. (2021). The leached Fe from each extraction was determined by Atomic Absorption Spectrometry (AAS). Pyrite iron was calculated from pyrite sulfur, which was extracted using the $CrCl_2$ reduction method

and precipitated as Ag_2S in silver nitrate traps (Canfield et al. 1986). Pure pyrite standards (Alfa Aesar) were used to monitor Fe recovery (93.8% ± 1.9%, $n = 5$). Three internal shale standards (CUG-4, CUG-6, and CUG-7) were measured during the extraction of all samples. Residual Fe concentrations were calculated as the difference between total Fe and Fe_{HR} concentrations.

2.3 | Thallium Isotope Compositions

Authigenic Tl was separated from detrital-bound Tl via an established partial leaching technique (Nielsen et al. 2011; Owens et al. 2017). This method is used because detrital Tl can obscure $\varepsilon^{205}Tl_{seawater}$ signals recorded in the authigenic fraction of anoxic sediments. Approximately 100 mg of powdered material from each shale sample was leached in either 2 M HNO_3 or concentrated HNO_3 at 130°C for 12 h to selectively dissolve Fe sulfides and sulfide-bound Tl. The isotopic compositions of modern anoxic sediments treated with either HNO_3 concentration are indistinguishable from modern $\varepsilon^{205}Tl_{seawater}$, suggesting chemical separation of the authigenic phase in either case (Fan et al. 2020; Nielsen et al. 2011; Owens et al. 2017). The resulting supernatant was separated via centrifugation and dried down before treatment with a series of aqua regia (3:1 HCl and HNO_3), inverse aqua regia (1:3 HCl and HNO_3), and $HNO_3 + H_2O_2$ digestions that break down organic matter extracted with the authigenic Tl. Samples were redissolved in 1 mL 1 M HCl and 1% by volume bromine-saturated water (hereafter H_2O-Br_2). The H_2O-Br_2 ensures full oxidation from Tl(I) to Tl(III), which allows Tl to form anionic complexes with the halogens that adhere strongly to the anion exchange resin used during ion exchange chromatography (Matthews and Riley 1969).

Two sets of ion exchange chromatography columns were performed to purify Tl from the sample matrix following previously published methods (Nielsen et al. 2004; Owens et al. 2017). In the first round of purification, glass columns were loaded with 1 mL anion exchange resin (AG1-X8) and cleaned with 0.1 M HCl with 5% by weight dissolved SO_2. Samples were loaded onto the columns, and the sample matrix was eluted using 15 mL of 0.5 M HNO_3, 2.0 M HNO_3, and 0.1 M HCl, with brominated water added in each step to maintain the trivalent state of Tl and its adherence to the resin. Thallium was then reduced and eluted from the resin using 15 mL 0.1 M HCl with 5% dissolved SO_2. The second round of columns was identical to the first but performed in mini Teflon columns that used a tenth of the resin and acid volumes.

Thallium isotope ratios were quantified with a Thermo Neptune multiple collector inductively coupled plasma mass spectrometer (MC-ICP-MS) housed at the Woods Hole Oceanographic Institution (WHOI) Plasma Facility. Standard-sample bracketing and external normalization to NIST SRM 981 Pb were applied to correct for instrumental mass bias. As a known amount of Pb was added to each sample, authigenic Tl concentrations could be calculated from the measured $^{205}Tl/^{208}Pb$ (Nielsen et al. 2004, 2015). USGS SCo-1 shale reference material was analyzed with each sample set to monitor instrumental accuracy and reproducibility, with an average $\varepsilon^{205}Tl$ of −2.9 ± 0.2‰; 2SD ($n = 3$), which was within error of values reported in previous work (−2.9 ± 0.1‰; 2SD; Ostrander et al. 2017).

3 | Results

All data are presented in Figures 2 and 3 and are available in the Supporting Information (Table S1). Authigenic Tl in the Qingjiang section exhibits slight variability across the profile, with authigenic concentrations ranging from ~1 to 5 μg/g and isotope compositions ranging from $\varepsilon^{205}Tl = -2.1$ to −4.5‰. These samples yield a wide range of Mo_{EF} (1–112), U_{EF} (1–17), and V_{EF} (1–15). Qingjiang samples show elevated but variable Fe_{HR}/Fe_T (0.41–1) and Fe_{py}/Fe_{HR} (0.37–0.85), with the former decreasing in younger samples.

Samples from the Weng'an section exhibit similar variability in authigenic Tl concentrations and isotope compositions, ranging from 0.2 to 3 μg/g and −2.3 to −4.2‰, respectively. Samples exhibit slightly higher RSE enrichment, with Mo_{EF} ranging from 1 to 178, U_{EF} ranging from 1 to 53, and V_{EF} ranging from 1 to 54. Thallium isotope compositions are broadly stable around −3 to −4‰ throughout both sections (Figure 3). Though the isotope compositions vary slightly across the study interval and appear to increase in younger samples, $\varepsilon^{205}Tl_{auth}$ before and after the Qingjiang biota interval are not significantly different in either section (Welch's t-test, Qingjiang: $p = 0.13$, $t = -1.6$, df = 11.7; Weng'an: $p = 0.35$, $t = -1.1$, df = 3.1). In the Qingjiang core, RSE enrichments gradually decrease in younger samples, with a notable decrease in authigenic Tl concentrations after the Qingjiang biota interval from an average of 1.4 μg/g Tl to 0.25 μg/g Tl. In the Weng'an section, authigenic Tl, Mo_{EF}, U_{EF}, and V_{EF} are broadly homogenous before the Qingjiang biota interval, after which values similarly show a marked decrease.

4 | Discussion

4.1 | Local Redox in the Nanhua Shelf Environment

Seawater $\varepsilon^{205}Tl$ capture is most effective in sediments today with reducing porewaters (Fan et al. 2020; Owens et al. 2017; Wang et al. 2022). Hence, other methods must first be used to constrain the local redox conditions of the Yangtze Platform shelf. In the shallower Qingjiang section, moderate to high enrichments in redox-sensitive elements (RSE) and Fe_{HR}/Fe_T values well above 0.38 suggest a persistently anoxic depositional environment throughout Cambrian Ages 2 and 3 (Algeo and Tribovillard 2009; Poulton and Canfield 2011). Values for Fe_{Py}/Fe_{HR} vary between 0.65 and 0.8 and suggest that the water column was euxinic (i.e., contained free sulfide in the water column), or was intermittently euxinic, in strata older than the Qingjiang biota, but these conditions likely gave way to ferruginous (anoxic with dissolved Fe in the water column) conditions coincident with their appearance (Figure 2). Elevated Mo_{EF} relative to U_{EF} throughout the interval evidence the formation of Fe-Mn oxyhydroxide particles that shuttle Mo from surface waters to anoxic bottom waters/sediments (Figure 4), as has been suggested to occur elsewhere in the Nanhua Basin (Cheng et al. 2017; Han et al. 2018; Li et al. 2021). In this scenario, the precipitation of Fe-Mn (hydr)oxide phases in

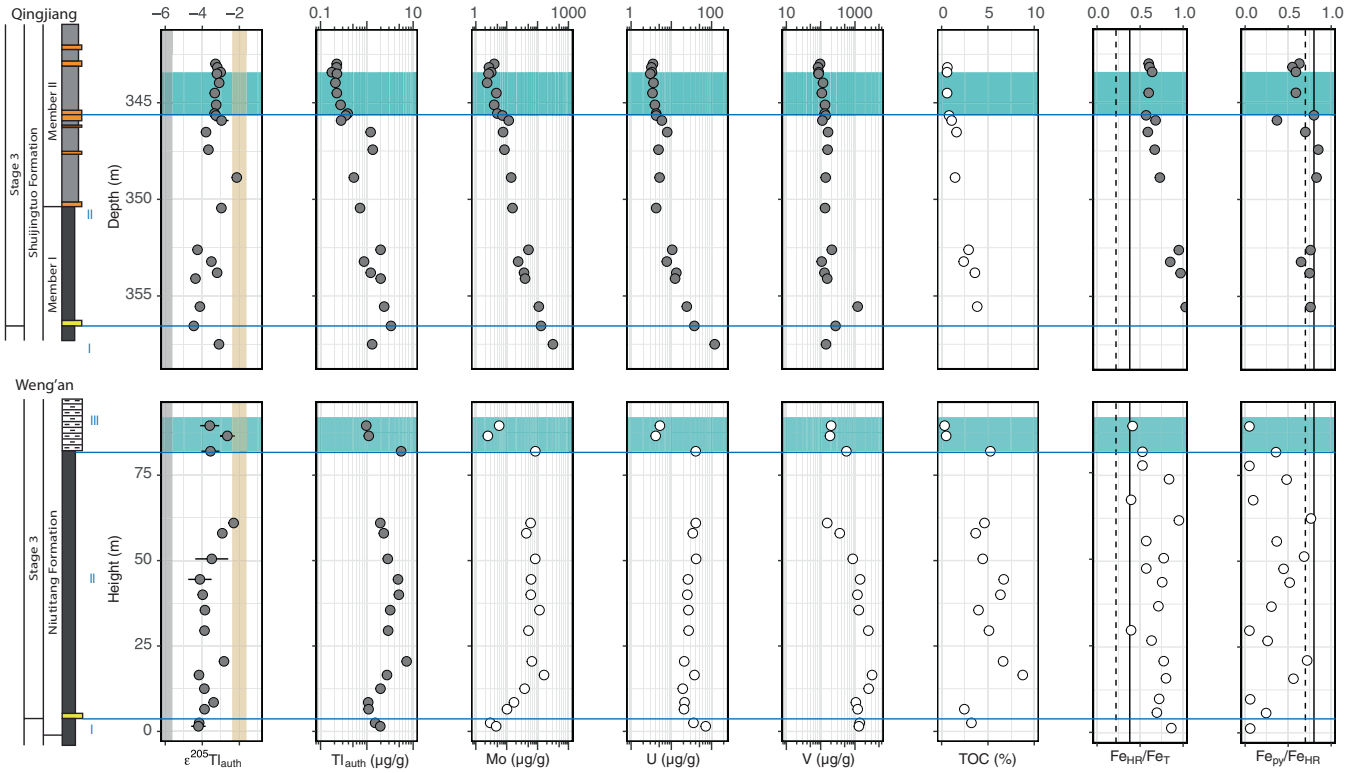

FIGURE 2 | Authigenic $\varepsilon^{205}Tl$, trace element concentrations, and Fe-speciation data for the lower Cambrian in the Qingjiang (top) and Weng'an (bottom) sections. Data generated in this study are shown in grey; previously published data are shown in white. Blue lines divide correlated intervals I-III. Qingjiang biota first appeared during the interval highlighted with a teal bar in Interval III. Error bars represent ±2SD of multiple sample analyses or the long-term reproducibility of SCo-1, whichever is greater. Vertical bars mark the average $\varepsilon^{205}Tl$ of modern seawater (gray) and bulk crust (brown). Vertical lines in the Fe_{HR}/Fe_T and Fe_{py}/Fe_{HR} plots mark the thresholds for anoxic ($Fe_{HR}/Fe_T > 0.22–0.38$) and euxinic ($Fe_{py}/Fe_{HR} > 0.7–0.8$) conditions, respectively (Poulton and Canfield 2011). Fe-speciation data are not available for samples targeted for $\varepsilon^{205}Tl$ measurements in the Weng'an section, but previously published measurements for other samples in the same section are shown (Jin et al. 2016). Trace element and TOC data for the Weng'an section are from Han et al. (2018). TOC data for the Qingjiang section are from Fan et al. (2023). Note the logarithmic scale for Tl_{auth}, Mo, U, and V concentrations.

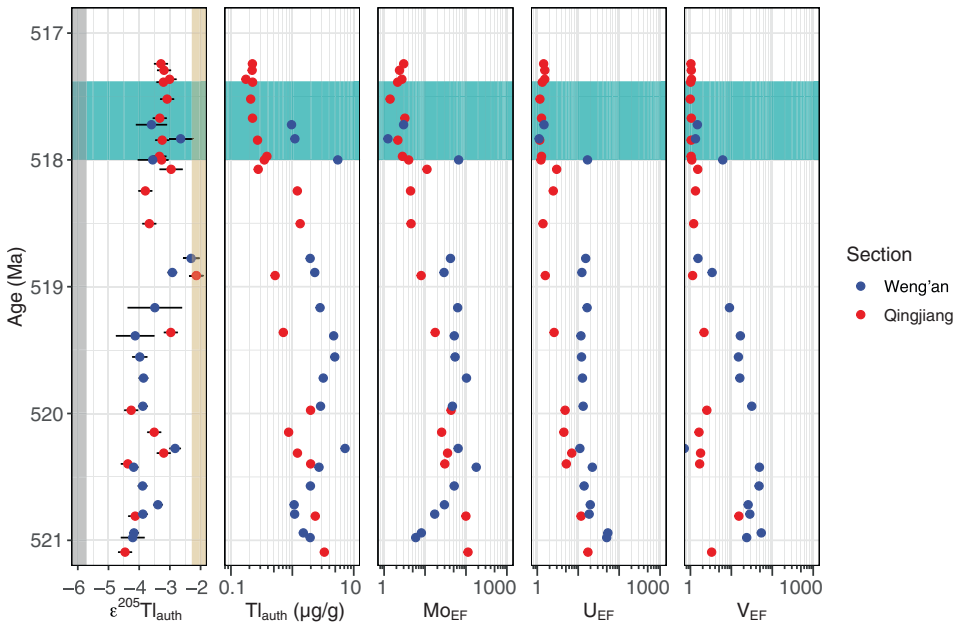

FIGURE 3 | Integrated profiles for Tl_{auth} and Mo, U, and V enrichment factors across lower Cambrian Stage 3 from the Weng'an (blue) and Qingjiang (red) sections. Qingjiang biota first appeared during the highlighted teal interval (> 518 Ma). Error bars represent ±2 SD of multiple sample analyses or the long-term reproducibility of SCo-1, whichever is greater. Vertical bars mark the average $\varepsilon^{205}Tl$ of modern seawater (gray) and bulk crust (brown).

oxic surface waters would have readily adsorbed molybdate and served as a vector to transport Mo below the chemocline. Although these oxides will reductively dissolve in anoxic bottom waters, sulfides can recapture liberated Mo to enrich anoxic sediments with authigenic Mo (Scholz et al. 2013). Such shuttling is evidenced in the Black Sea today but with no effect on sedimentary ε^{205}Tl values (Chen, Li, et al. 2022). These data considered, it is likely that the sediments in the Qingjiang site were deposited under anoxic conditions that were conducive to recording $\varepsilon^{205}Tl_{seawater}$.

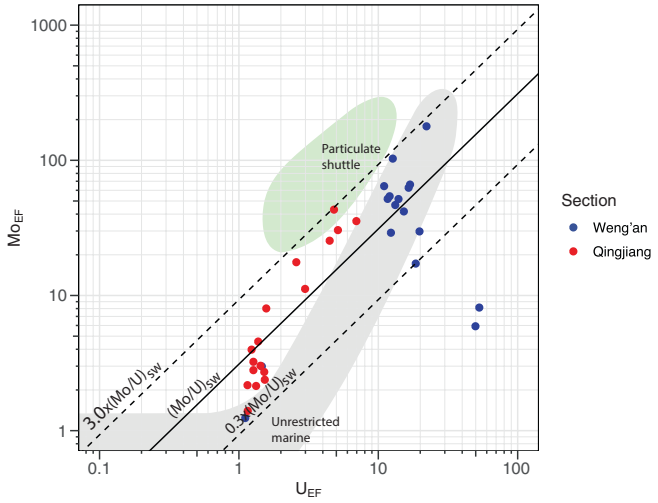

FIGURE 4 | Cross-plot of sedimentary Mo and U enrichment factors (EFs) for the Weng'an (blue) and Qingjiang (red) sections. The green and gray fields highlight expected Mo_{EF}-U_{EF} values for sediments in unrestricted marine settings and under sites of intense redox cycling of Fe-Mn oxide particles, respectively. Diagonal lines represent multiples (3, 1, and 0.3) of the Mo/U value of modern seawater (after Algeo and Tribovillard 2009 and Tribovillard et al. 2012). Note the logarithmic scale in both axes.

In the outer shelf Weng'an section, Mo and U enrichments imply a more variable redox history. Previously published Fe speciation data from the outcrop track a broadly anoxic water column with phases of sulfide accumulation and possibly oxygenated conditions, particularly during the appearance of the Qingjiang biota (fig. 2; Jin et al. 2016). A detailed redox history of the Weng'an section is beyond the scope of this work, but we conclude that the outcrop was sufficiently anoxic throughout the study interval to record $\varepsilon^{205}Tl_{seawater}$ based on several observations. In line with the Fe_{HR}/Fe_T values above the anoxic threshold observed by Jin et al. (2016; Figure 2), high enrichments in Mo, U, V, and TOC point to deposition under anoxic and possibly sulfidic conditions. Furthermore, Al-normalized V/Mo and U/Mo ratios are similar to those found in sediments within modern OMZ settings (Figure 5).

After ~518 Ma, RSE and TOC values drop sharply. However, if these changes signal an oxygenation of outer-shelf porewaters sufficient to prevent $\varepsilon^{205}Tl_{seawater}$ capture, then $\varepsilon^{205}Tl_{auth}$ would be expected to shift to values as heavy as ~ +10‰ associated with Mn oxide formation (Rehkämper et al. 2002; Wang et al. 2022). Thallium isotope compositions are instead stable at $\varepsilon^{205}Tl \approx -3.5$‰. Importantly, even oxic depositional environments are capable of capturing $\varepsilon^{205}Tl_{seawater}$ if pore waters rapidly become anoxic (Wang et al. 2022), implying no inconsistency between previous work on local redox conditions after ~518 Ma in the Weng'an section (Jin et al. 2016) and our Tl isotope data. We further note that the Weng'an ε^{205}Tl record shows strong congruence with that of the Qingjiang section throughout the study interval (Figure 3), such that both redox environments were likely similarly conducive to capturing $\varepsilon^{205}Tl_{seawater}$. We argue it is therefore likely that both the Qingjiang and Weng'an sections record the contemporaneous ε^{205}Tl value of the overlying water column.

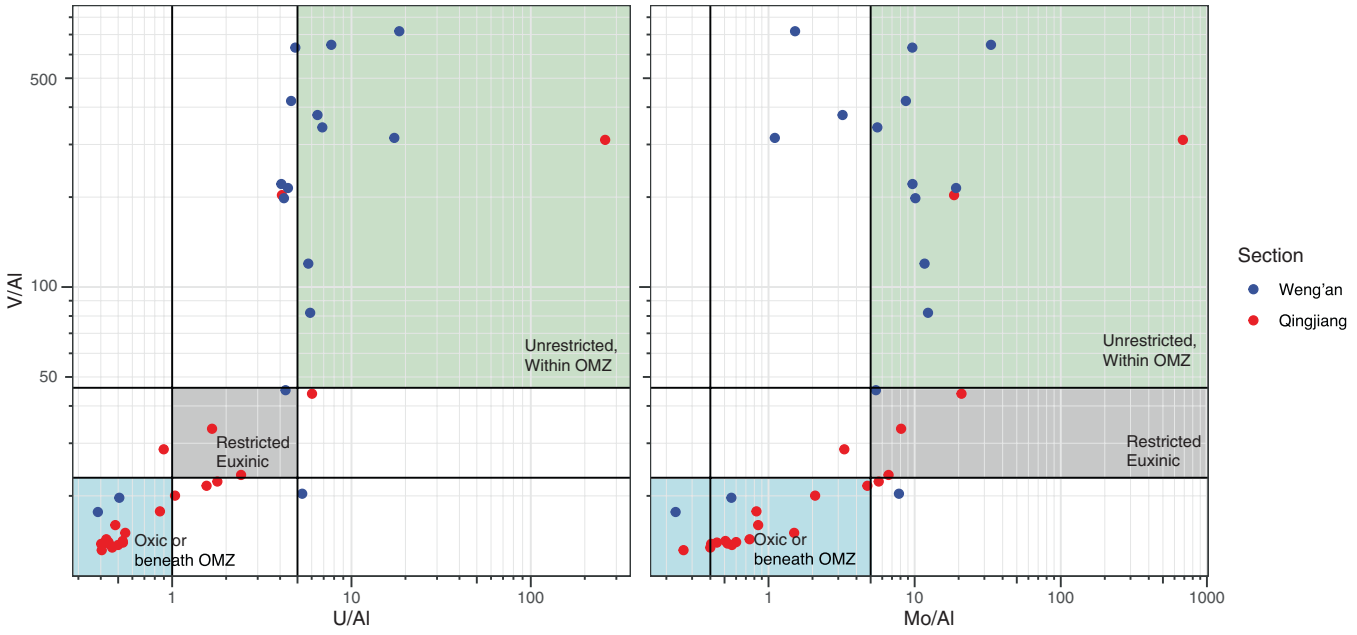

FIGURE 5 | Cross-plots of Al-normalized U (left) and Mo (right) against Al-normalized V, with labeled/colored fields for the expected values of different depositional environments (after Bennett and Canfield 2020). Note the logarithmic scale in both axes.

4.2 | Open-Ocean Connectivity in the Nanhua Basin

If the Nanhua Basin was a semi-isolated basin during the formation of the studied shales, then reconstructed $\varepsilon^{205}Tl_{seawater}$ values could be a strictly local signature. This happens in semi-isolated basins today because the majority of Tl supplied to these basins does not come from the open ocean, but instead from local riverine or anthropogenic sources (e.g., the Black and Baltic seas; Owens et al. 2017; Ostrander et al. 2024). Indeed, the influence of hydrographic restriction is an often-debated concern on the geochemistry of the Nanhua Basin: though South China was likely paleogeographically isolated and surrounded by the open ocean (Li et al. 2008), geochemical data have been used to infer at least partial restriction across the basin (e.g., Chen, Wang, and Jin 2022; Xu et al. 2012). Notably, this argument was used to reject a global interpretation of the $\varepsilon^{205}Tl_{auth}$ record in a slope setting of the Nanhua Basin during the early-middle Ediacaran (Ostrander et al. 2020). However, we first note that the samples in our Cambrian dataset were deposited at least ~30 My after those inferred to represent a time of basinal restriction in the Ediacaran; connectivity with the open ocean in the Cambrian does not necessarily contradict restriction in the Ediacaran. Within the Nanhua Basin, restricted conditions that record strictly local $\varepsilon^{205}Tl$ in the Ediacaran are marked by extremely low Mo and U concentrations of a few μg/g (Ostrander et al. 2020). In contrast, higher concentrations of Mo and U in our record more closely reflect values from purported times of connectivity in the Ediacaran and seem to require stronger seawater Mo and U inputs (Algeo and Tribovillard 2009). Other observations from the Nanhua Basin support at least partial connection with the open ocean during this time: black shale deposits and fossil assemblages in sections of the Yangtze Platform have been correlated with other deposits globally (Jin et al. 2020; Steiner et al. 2007), and trace element enrichments in slope sections near the outer shelf have been shown to suggest well-connected bottom waters (Wang et al. 2015; Wei et al. 2020). These data are particularly relevant to the Weng'an section that was deposited near these mid-slope sections, but the indistinguishable $\varepsilon^{205}Tl$ values throughout the two sections suggest similar interpretations for the connectivity of the basin.

While the data are inconsistent with extreme restriction comparable to the modern Black Sea, it is possible that our $\varepsilon^{205}Tl$ record reflects conditions more analogous to modern basins with greater, albeit still limited, connection with the open ocean. For instance, in the modern Baltic Sea, links to global-ocean chemistry are limited to sporadic inflow events from the North Sea (Matthäus et al. 2008) such that the pre-industrial $\varepsilon^{205}Tl_{auth}$ of ~ −4‰ represents a mix of riverine ($\varepsilon^{205}Tl = -2$‰) and open-ocean ($\varepsilon^{205}Tl = -6 \pm 0.3$‰) Tl inputs (Ostrander et al. 2024). An average $\varepsilon^{205}Tl$ of ~ −4‰ in the Nanhua Basin during the Cambrian could analogously represent some mix of riverine and open-ocean waters with an unknown isotope composition lighter than −4‰.

If $\varepsilon^{205}Tl_{auth}$ variability was driven by rates of water-mass exchange with the open ocean, RSE enrichment should correlate with $\varepsilon^{205}Tl_{auth}$ as increased connectivity replenished the Mo, U, V, and Tl reservoirs of the basin. Indeed, in the Qingjiang section, $\varepsilon^{205}Tl_{auth}$ is significantly and moderately correlated with Tl_{auth}, and in the Weng'an section, it is significantly correlated with V_{EF} (Table 1). These trends may well indicate some influence of partial basin restriction.

Supporting this interpretation, gradual declines in RSE enrichments in the Qingjiang section could signal their depletion from insufficient renewal (Figure 3). This is particularly relevant for V, which has been shown to be more sensitive to reservoir depletion during recent periods of limited seawater exchange in the turbid Baltic Sea; this sensitivity may be echoed in the notably low enrichments of V compared to Mo and U throughout the Qingjiang record (Figure 3).

However, several other lines of evidence more strongly support a negligible riverine signal in the Tl isotope mass balance of the Nanhua Basin. First, the absence of similarly significant and strong correlations in the opposite sections (i.e., between $\varepsilon^{205}Tl_{auth}$ and Tl_{auth} in Weng'an and between $\varepsilon^{205}Tl_{auth}$ and V_{EF} in Qingjiang data) despite broadly congruent $\varepsilon^{205}Tl_{auth}$ trends at both sites suggests that these unique relationships may not signal basin-wide controls on Tl and other RSE cycling. Furthermore, most other RSE correlations with $\varepsilon^{205}Tl_{auth}$ are either statistically insignificant or only explain a minimal fraction of its variability (Table 1).

In the deeper-water Weng'an section, covariations in Mo_{EF}-U_{EF}, Al-normalized V-Mo, and Al-normalized V-U are all similar to those found in sediments of modern, unrestricted settings (Figures 4 and 5). In the shallower Qingjiang section, Mo_{EF}/U_{EF} trends similarly reflect those of a modern, open-marine setting (Figure 4), albeit with slightly higher Mo enrichments possibly driven by Fe-Mn shuttling. Vanadium/Mo and V/U values

TABLE 1 | Summary of linear regression statistics between $\varepsilon^{205}Tl_{auth}$ and (log-transformed) redox-sensitive element enrichments.

Section	*p*	Adjusted R^2
Combined		
Mo_{EF}	0.082	0.056
U_{EF}	**0.036**	**0.092**
V_{EF}	**0.00051**	**0.27**
Tl_{auth}	**0.0050**	**0.18**
Qingjiang		
Mo_{EF}	0.17	0.049
U_{EF}	0.30	0.0072
V_{EF}	0.178	0.046
Tl_{auth}	**0.00064**	**0.44**
Weng'an		
Mo_{EF}	0.50	0
U_{EF}	0.069	0.15
V_{EF}	**0.00015**	**0.63**
Tl_{auth}	0.76	0

Note: Bolded values indicate statistically significant correlations ($p < 0.05$).

are notably lower in the Qingjiang section than in the Weng'an section, but these RSE trends nonetheless mirror those of sediments beneath modern OMZs in unrestricted, continental margin settings (fig. 5; Bennett and Canfield 2020). Although low Mo/TOC values in both sections may suggest higher degrees of restriction relative to the modern Baltic Sea (Figure 6), such values more likely reflect a reduced global marine Mo reservoir in the Cambrian—an expected consequence of more widespread anoxia and reduced oxidative weathering in the early Paleozoic landscape (e.g., Sperling, Wolock, et al. 2015; Dahl et al. 2017).

Akin to the modern Baltic Sea, a riverine input sufficient to affect the Tl isotope composition of the Nanhua Basin should be reflected in low-salinity or brackish conditions. While the salinity of the region during the Cambrian remains debated, recent studies suggest that deeper Nanhua Basin seawater either (1) was similar to marine conditions throughout the study interval (Zhang et al. 2023) or (2) transitioned from brackish to marine conditions with increasing exchange with the open ocean (Cheng et al. 2023). In the former scenario, seawater $\varepsilon^{205}Tl$ is straightforwardly equal to that of the open ocean. In the latter scenario, decreasing relative riverine input, presumably with a crustal Tl isotope composition (−2‰), would be expected to yield increasingly lighter $\varepsilon^{205}Tl_{auth}$, yet this is not observed in the $\varepsilon^{205}Tl$ record (Figures 2 and 3). Taken together, the data are more consistent with a minimal effect of restriction on our Tl isotope record.

4.3 | Alternate Drivers of $\varepsilon^{205}Tl$ Trends

Alternatively, authigenic $\varepsilon^{205}Tl$ values may have been altered through early diagenesis or later-stage processes, such as weathering of the Weng'an outcrop. In the former scenario, it is unlikely that remobilization would have altered $\varepsilon^{205}Tl$ values, as seawater Tl is rapidly removed into sediments under anoxic conditions and would not be significantly remobilized in a largely anoxic diagenetic environment (Ahrens et al. 2021). Any addition of Tl from porewaters would likewise have a minimal effect, as diagenetic fluid Tl concentrations, on the order of a few pg/g, are much lower than the few μg/g authigenic Tl concentrations of the sediment. Though the effects of later-stage alteration (e.g., weathering) on Tl isotopes have not been constrained, the general congruence between the $\varepsilon^{205}Tl$ trends of the outcrop (Weng'an) and core (Qingjiang) sections (Figure 3) is consistent with limited alteration.

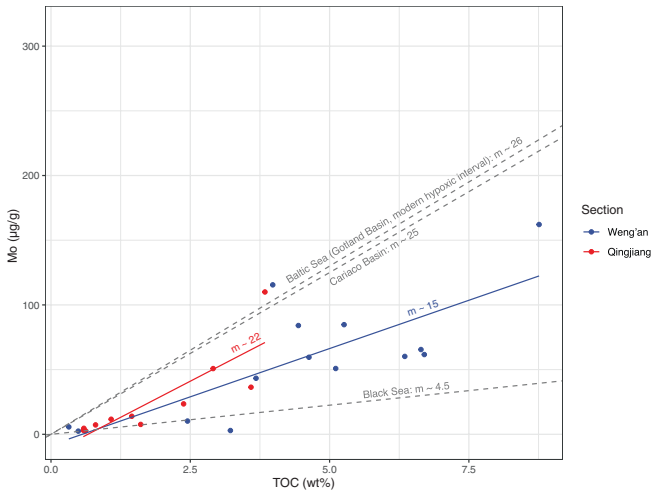

FIGURE 6 | Sedimentary Mo-TOC data for the Weng'an (blue) and Qingjiang (red) sections. The slope m of the best-fit line is compared to the slopes of previously studied restricted basins, with higher slopes inversely correlated with restriction (Cariaco Basin and Black Sea: Algeo and Lyons 2006; Baltic Sea: Van Helmond et al. 2018).

4.4 | Global Redox Across the Cambrian Explosion

Contrary to previous suggestions of a shift to near-modern extents of marine oxygenation during Cambrian Age 3 (Chen et al. 2015; Li et al. 2021; Wen et al. 2015), the new Tl isotope data do not record modern extents of marine oxygenation as evidenced by modern Tl isotope compositions either following the ~521 Ma Stage 2–3 boundary or during the appearance of the Qingjiang biota at ~518 Ma. Instead, invariant and lighter-than-crustal $\varepsilon^{205}Tl_{auth}$ support two straightforward, alternative interpretations: (1) deep-ocean redox conditions were broadly stable but less oxygenated than the modern ocean, and (2) the diversification of the Qingjiang biota was not accompanied by a dramatic change in deep seafloor oxygenation. Our data do not support claims of near-modern global deep-ocean oxygenation to permit rapid radiation of metazoan radiation near the Age 2–3 boundary.

Although lower Cambrian shale $\varepsilon^{205}Tl_{auth}$ do not approach the modern seawater value, they are noticeably lower than the overwhelmingly near-crustal values found in the Ediacaran shale record (Ostrander et al. 2020, 2023). The Tl isotope compositions in our dataset show clear deviations from crustal values ($\varepsilon^{205}Tl \approx -2$‰) to compositions as light as $\varepsilon^{205}Tl \approx -4.5$‰. These values are significantly lower than the isotopic compositions measured for the Ediacaran from multiple basins (average $\varepsilon^{205}Tl_{auth} = -3.5 \pm 0.6$‰, $n = 38$ in the early Cambrian compared to -2.2 ± 0.7‰ in the Ediacaran, $n = 113$, Welch's t-test, $p < 2.2 \times 10^{-16}$, $t = -11.2$, df = 82.5, Figure 7). Interpreted straightforwardly (i.e., that a lower $\varepsilon^{205}Tl_{auth}$ is driven by increased Mn oxide burial from increased oxygenation), the $\varepsilon^{205}Tl$ decrease observed across the Ediacaran–Cambrian boundary could well indicate some amount of increased oxygenation. However, given the ~40 My gap between the samples of this study and the youngest samples from Ediacaran Tl isotope datasets, the exact timing and extent of the shift to more oxygenated conditions cannot be determined by the present datasets. More work is required to identify the timing and tempo of this oxygenation.

4.5 | Reinterpreting Global Oxygenation

Ideally, other proxy data previously interpreted as evidence of global deep-ocean oxygenation must be reconciled with the comparatively anoxic oceans illustrated by our $\varepsilon^{205}Tl_{auth}$ record (Figure 8). Samples across the Stage 2–3 boundary record $\delta^{98}Mo$ values ranging from ~ −0.1 to ~ +2.3‰ (Chen et al. 2015) and $\delta^{238}U$ values ranging from ~ −1.0 to ~ −0.4‰ (Dahl et al. 2017; Wei et al. 2020). The most positive of these values are similar to modern seawater (modern $\delta^{98}Mo_{seawater} = 2.34$‰; modern $\delta^{238}U_{seawater} = -0.39 \pm 0.01$‰; Goldberg et al. 2013; Lau et al. 2019) and are straightforwardly interpreted or modeled as evidence for "modern-like" states of ocean oxygenation near the Cambrian Age 2–3 boundary—that is a broadly oxygenated

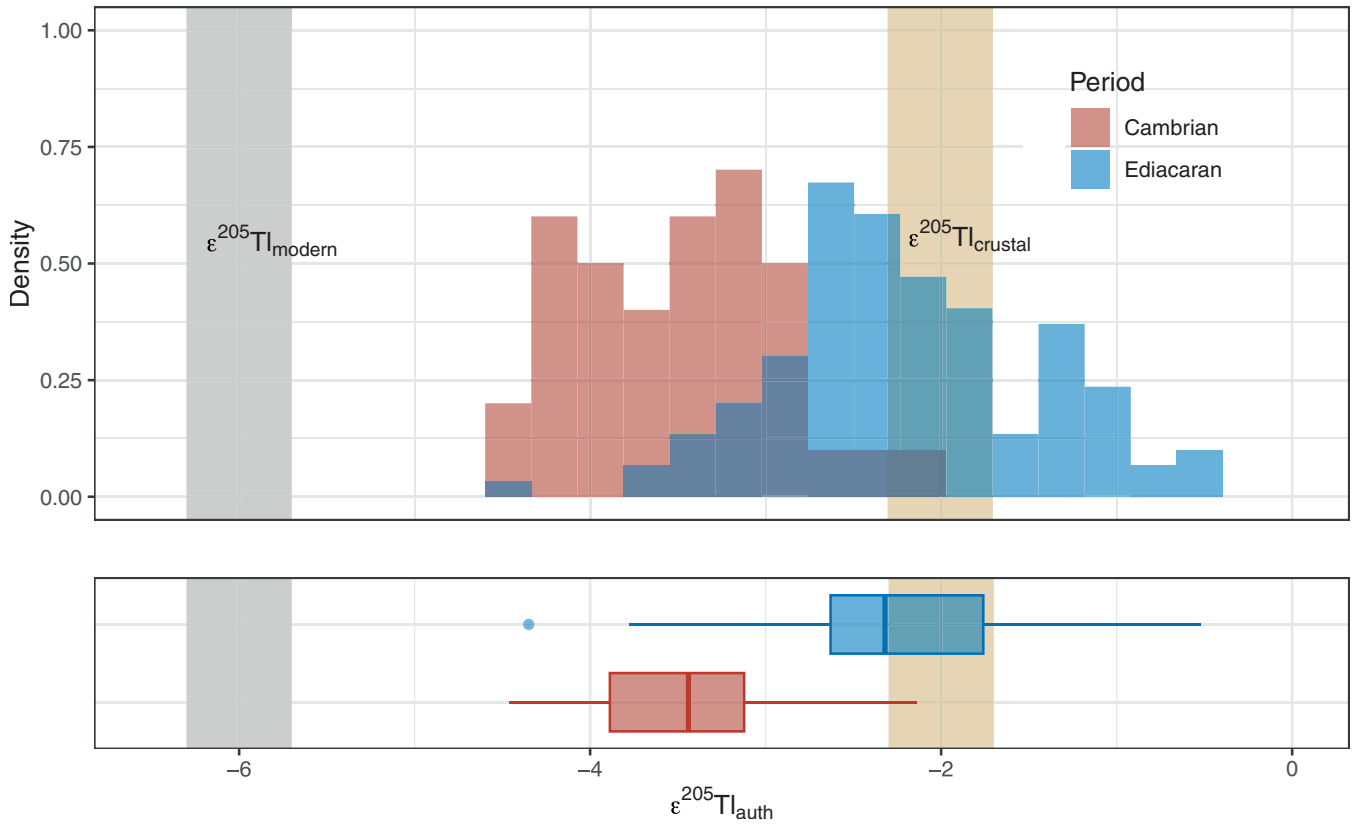

FIGURE 7 | Histogram (top) and boxplot (bottom) of $\varepsilon^{205}Tl_{auth}$ from this study (red) and Ediacaran samples (blue). Data for the Ediacaran are from Ostrander et al. (2020, 2023) excluding the data from shales inferred to have been deposited in a restricted basin.

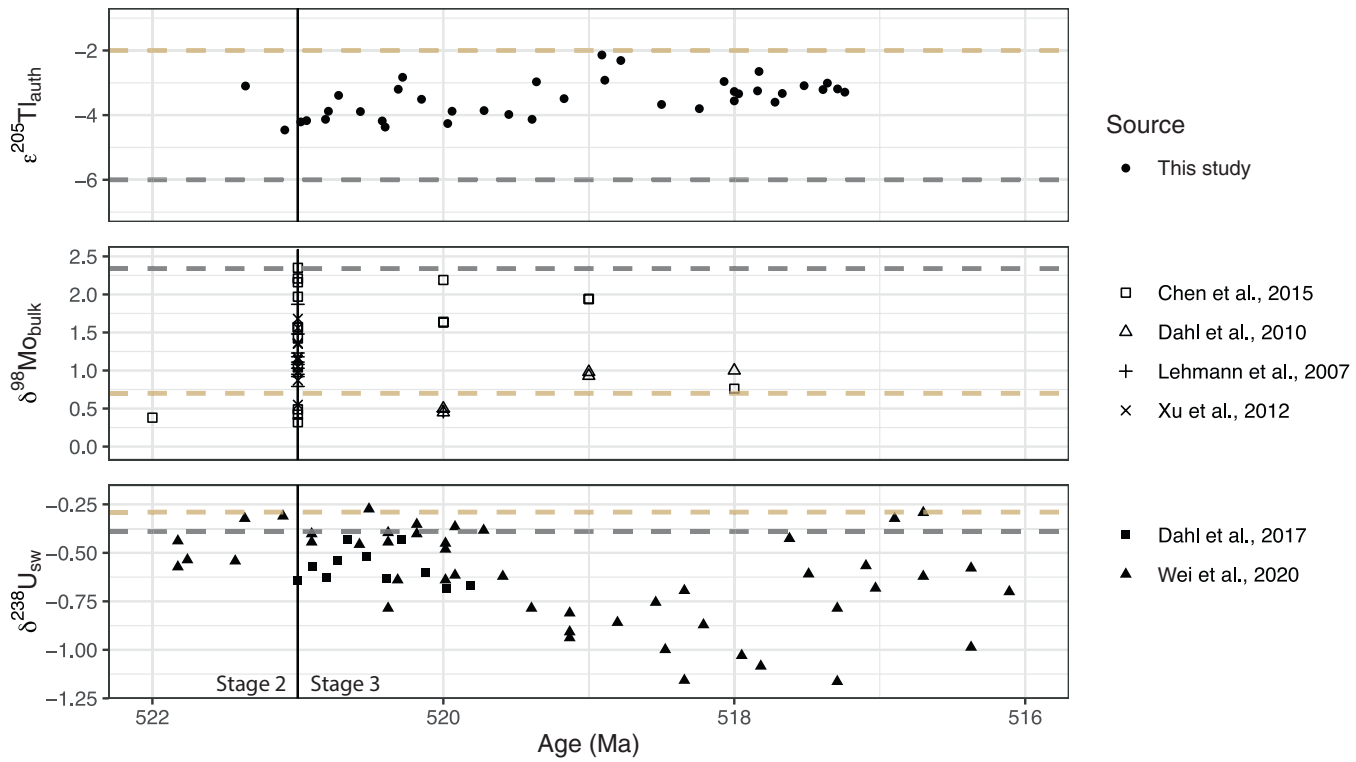

FIGURE 8 | Compilation of upper Stage 2 to lower Stage 3 $\varepsilon^{205}Tl_{auth}$, $\delta^{98}Mo_{bulk}$, and $\delta^{238}U_{sw}$ data. $\varepsilon^{205}Tl_{auth}$ are from this study, $\delta^{98}Mo_{bulk}$ are compiled by Chen et al. (2015), and $\delta^{238}U_{sw}$ are compiled and calculated from authigenic shale $\delta^{238}U$ by Wei et al. (2020). Dashed lines represent the isotope composition of modern seawater (gray) and crustal input (brown) for each isotope system.

deep ocean (Chen et al. 2015; Dahl et al. 2017; Li et al. 2021; Wen et al. 2015). However, several complexities hinder such straightforward interpretations.

A critical caveat to interpretations of the Mo isotope record is that no sink in the modern ocean captures Mo without fractionating its isotopes, and these sinks can only drive seawater $\delta^{98}Mo$ to values heavier than modern riverine inputs ($\delta^{98}Mo_{in} \approx 0.7‰$) because all sinks preferentially remove lighter-mass Mo isotopes (reviewed in Kendall et al. 2017). Thus, this complication implies that a sufficient change in the extent of any combination of sinks can, in theory, drive modern-like $\delta^{98}Mo$ without necessarily oxygenating the deep ocean. For instance, in the modern Baltic Sea, sediments formed under weakly euxinic settings that scavenge Mo non-quantitatively can exhibit $\delta^{98}Mo$ as negatively fractionated from waters as sediments formed under fully oxygenated settings (Nägler et al. 2011). Thus, a large positive $\delta^{98}Mo$ shift ~520 Ma may instead represent a transition from a dominant marine state with limited effective fractionation—such as broad, strongly euxinic conditions with quantitative Mo drawdown—to the expansion of these lower-H_2S conditions that impart "oxygenated-like" degrees of fractionation observed in the Baltic Sea today. In this scenario, contraction of strongly euxinic conditions could yield seawater $\delta^{98}Mo$ akin to that of the modern ocean without perturbing the marine Tl budget through deep-ocean oxygenation. Additionally, if water column stratification with oxic surface waters and anoxic bottom waters were globally relevant, it is also possible that broad extents of Fe-Mn shuttling would preferentially bury sufficient ^{95}Mo to drive heavier (more modern) seawater $\delta^{98}Mo$ while Tl isotopes remained unfractionated (Chen, Li, et al. 2022). Recent modeling efforts have shown that values similar to modern $\delta^{98}Mo_{seawater}$ require substantially lower extents of bottom-water oxygenation if Fe-Mn cycling is explicitly considered in mass-balance modeling of a broadly anoxic ocean with euxinic margins (Qin et al. 2022).

Complications also hinder direct conversion of near-modern sedimentary $\delta^{238}U$ into interpretations of near-modern extents of marine oxygenation. As with the Mo isotope record, near-modern U isotopic compositions only represent a fifth of the authigenic $\delta^{238}U$ values measured near the Stage 2–3 boundary; isotope compositions from the proposed $\delta^{238}U_{auth}$ excursion range from ~ −0.4 to −0.7‰ (see $\delta^{238}U$ compilation by Chang et al. 2023). This large range of data may stem from the fundamentally local redox processes that can offset $\delta^{238}U_{auth}$ from the isotopic composition of the overlying water column. Chiefly, $\delta^{238}U_{auth}$ in sediments formed under reducing settings like those inferred from Fe-speciation data in the shale $\delta^{238}U_{auth}$ record of the lower Cambrian (Wei et al. 2020) would be fractionated toward higher values during the reduction of U(VI) to U(IV) (reviewed in Lau et al. 2019) and must be corrected to infer contemporaneous seawater $\delta^{238}U$. This correction factor, however, can vary strongly with basin conditions (Lau et al. 2022). For instance, the fractionation-corrected, near-modern values deduced by Wei et al. (2020) invoked fractionation factors ranging from −0.15‰ to −0.8‰. Yet these corrected values are again among the most positive of shale samples near the Stage 2–3 boundary, and they, too, are higher than coeval $\delta^{238}U_{auth}$ values obtained from carbonates that themselves can be positively fractionated in reducing diagenetic pore fluids. With the assumption that more negative values at any time point therefore represent the composition closest to that of contemporaneous seawater, the lowest carbonate-hosted $\delta^{238}U_{auth}$ values near the Stage 2–3 boundary would reflect a seawater composition closer to −0.6 to −0.8‰. In the context of Cambrian oceans, this $\delta^{238}U$ would require a significantly smaller change in marine redox. Following the example of a global departure from strongly euxinic continental shelves, a more dominant ferruginous or weakly euxinic shelfal regime could yield a smaller (observed) positive fractionation (Andersen et al. 2014) and drive global U isotope compositions closer to modern values.

Recent work places further uncertainty in these $\delta^{238}U_{auth}$ conversions to $\delta^{238}U_{seawater}$. Some measurements in altered carbonates and anoxic, siliciclastic sediment suggest $\delta^{238}U_{auth}$ is not solely shifted to more positive values than those of the overlying water column (Cole et al. 2020; Hood et al. 2018). Thus, as with Mo, this ambiguity offers the possibility that a sufficient change in many combinations of sinks can explain modern-like $\delta^{238}U_{auth}$ (see a similar discussion by Gong et al. 2023 regarding uranium isotopes during the Ediacaran Shuram Carbon Isotope Excursion).

Altogether, these arguments demonstrate that the Mo and U isotope compositions observed during the lower Cambrian need not be driven by modern-like ocean oxygenation. Importantly, we note that while we argue against a broadly oxygenated deep ocean akin to today, the positively correlated trends in both Mo and U isotope compositions suggest some global ocean redox change was likely. If these variations were associated with variable organic matter availability in South China where these records are produced, $\delta^{98}Mo$ and $\delta^{238}U$ would be expected to be inversely correlated as Mo and U uptake became increasingly inefficient (through decreased porewater sulfate reduction and/or organic matter oxidation) and increasing effective fractionations drove diverging $\delta^{98}Mo$ and $\delta^{238}U$ values (Brüske et al. 2020). A positive shift in both isotope systems instead signals a global perturbation to their respective marine budgets (see a related argument by Kendall et al. 2020). Namely, the previously discussed contraction of shelfal euxinia in a nonetheless stably anoxic regime offers a potential link between invariant $\varepsilon^{205}Tl$ values and possible perturbations in seawater Mo and U isotope compositions. Taken straightforwardly, the Fe-speciation data in this study chronicle a weak change in the redox environment of the shelf; decreasing Fe_{HR}/Fe_T values over 521–518 Ma and a shift to lower Fe_{py}/Fe_{HR} values ~518 Ma may reflect a transition from euxinic to ferruginous conditions in the local shelf and a broader increase in oxidation across early Age 3. These changes are broadly coeval with highly fluctuating, and generally contracting, extent of euxinia on the continental shelf in the Nanhua Basin (Cheng et al. 2016; Feng et al. 2014; Jin et al. 2016; Li et al. 2017; Xu et al. 2012) and overall elevated surface to mid-depth oxidation (Fan et al. 2023; Jin et al. 2016; Li et al. 2017). Evidently, Age 3 oxygenation could have occurred, but would have been limited in extent or depth to not perturb the marine Tl budget.

4.6 | Oxygenation and the Cambrian Explosion

The Tl isotope record suggests that the appearance of the Qingjiang biota ~518 Ma, and the broader exponential increase

in metazoan diversity ~521 Ma, occurred in a time of relatively stable deep-ocean redox conditions with limited (i.e., not modern) extents of oxygenation. These inferences suggest that neither the global extent nor a dramatic expansion of modern-like moderately or strongly oxygenated seafloor, at least on a scale to drive major changes in $\varepsilon^{205}Tl_{seawater}$, were permissive thresholds to metazoan radiation and diversification. As such, increased oxygenation to fully modern extents was unlikely to have been required for Cambrian-style animal body plans, and it is more likely that critical oxygen thresholds were much lower (Sperling et al. 2013, Sperling, Knoll, and Girguis 2015).

In this light, it is intriguing that early Cambrian oceans may have been characterized by some degree of oxic seafloor expansion relative to the Ediacaran (Figure 7). Although it is difficult to translate the observed change in Tl isotopes between the Ediacaran and Cambrian Stage 2–3 into a specific change in atmospheric oxygen given current modeling approaches, these results would probably signal minor global oxygenation. This inference would be consistent with recent suggestions by Stockey et al. (2024) that minor increases in atmospheric oxygen and marine productivity occurred around the Ediacaran–Cambrian boundary interval. Such minor oxygenation would have increased oxygen partial pressures in shelfal environments, where the majority of animals (both modern and Cambrian) live, while being insufficient to oxygenate the deep ocean to extents comparable to today. The nature and timescale of the statistical modeling in that study, however, did not allow for precise estimation of when this oxygenation occurred. Combining our Cambrian results with those of Ostrander et al. (2020, 2023), the Tl isotope record seems to suggest that a rise in ocean oxygenation occurred sometime between ~555 Ma and 521 Ma. Though increased oxygenation of the shelfal environments was likely more important for Cambrian diversification, our Tl record cannot rule out the possibility of less-than-modern accumulations of O_2 in the deep sea.

Considerable questions remain in demonstrating that such oxygenation was a causal trigger for the Cambrian explosion. From a data perspective, the late Ediacaran and Fortunian remain unstudied with respect to Tl isotopes, as are the remainder of the middle and later Cambrian. Higher temporal resolution on the timing of the Tl isotope shift is required. From the perspective of "permissive environments" hypotheses, it must be demonstrated that this represents a persistent shift away from the predominantly crustal values that define the Ediacaran and the first metazoan body fossils of the Ediacaran biota, as the appearance of modern animal body plans is subsequently stable on a Phanerozoic timescale. Given that the Tl isotope shift appears minor, and considering the statistical relationships between effect size, sample size, and power, it is likely that a large number of measurements will be required to fully resolve this signal. This is especially true if there is any cyclicity in the Tl isotope record, as with C isotopes (e.g., Smith et al. 2016) or U isotopes (e.g., Wei et al. 2020); note though that if the deep ocean remained anoxic through this interval, there may not be any Tl isotope cyclicity. From an ecophysiological perspective, it is necessary to link Tl geochemical results to the direct parameter that matters to animals, namely the partial pressure of oxygen in shallow shelf environments. Finally, from an evolutionary point of view, it is still unknown what represents an acceptable or expected temporal gap between oxygenation (and the advent of a permissive environment) and the appearance of new animal body plans. This is especially true if the appearance of disparate body plans is driven not by oxygenation itself, but by ecological factors such as the evolution of carnivory (Sperling et al. 2013). Nonetheless, at present, the Tl isotope record supports a minor oxygenation event sometime between the latest Ediacaran and the Cambrian explosion, with a magnitude that likely crossed critical ecological thresholds for early animal communities.

5 | Conclusions

We interpret the global marine redox environment using Tl isotope compositions from two shelf sections in the Nanhua Basin across the appearance of the Qingjiang biota ~518 Ma, which chronicles a particularly rapid interval of metazoan diversification and radiation in the broader Cambrian explosion. Depositional conditions (namely, local anoxia and basin connectivity with the open ocean) indicate the two sections likely recorded contemporaneous global $\varepsilon^{205}Tl_{seawater}$ and therefore reflect the state of global ocean oxygenation. Invariant $\varepsilon^{205}Tl_{auth}$ values from the Cambrian Stage 2–3 boundary (~521 Ma) through the Qingjiang biota interval (~518 Ma) suggest that the exponential increase in animal diversity in this interval was not associated with either a dramatic oxygenation event or the appearance of a modern-like ocean redox state, characterized by broad extents of moderately or strongly oxic seafloor. Rather, contemporaneous Mo and U isotope compositions can be reinterpreted as evidence of relatively limited oxygenation, such as on the continental shelves. Authigenic $\varepsilon^{205}Tl$ measured from the Cambrian are slightly more negative than in the Ediacaran, suggesting a minor expansion of oxic depositional environments from the late Ediacaran to the early Cambrian. However, this oxygenation was likely more dominant on continental shelves, which may have played a large role in triggering biotic innovation.

Conflicts of Interest

The authors declare no conflicts of interest.

Data Availability Statement

All data generated for this study are found in the Supporting Information of this article (Table S1).

References

Ahrens, J., M. Beck, P. Böning, et al. 2021. "Thallium Cycling in Pore Waters of Intertidal Beach Sediments." *Geochimica et Cosmochimica Acta* 306: 321–339.

Algeo, T. J., and T. W. Lyons. 2006. "Mo-Total Organic Carbon Covariation in Modern Anoxic Marine Environments: Implications for Analysis of Paleoredox and Paleohydrographic Conditions: Mo-TOC Covariation in Anoxic Sediments." *Paleoceanography* 21: e2006PA001016.

Algeo, T. J., and N. Tribovillard. 2009. "Environmental Analysis of Paleoceanographic Systems Based on Molybdenum–Uranium Covariation." *Chemical Geology* 268: 211–225.

Andersen, M. B., S. Romaniello, D. Vance, S. H. Little, R. Herdman, and T. W. Lyons. 2014. "A Modern Framework for the Interpretation of

238U/235U in Studies of Ancient Ocean Redox." *Earth and Planetary Science Letters* 400: 184–194.

Bennett, W. W., and D. E. Canfield. 2020. "Redox-Sensitive Trace Metals as Paleoredox Proxies: A Review and Analysis of Data From Modern Sediments." *Earth-Science Reviews* 204: 103175.

Brüske, A., S. Weyer, M.-Y. Zhao, et al. 2020. "Correlated Molybdenum and Uranium Isotope Signatures in Modern Anoxic Sediments: Implications for Their Use as Paleo-Redox Proxy." *Geochimica et Cosmochimica Acta* 270: 449–474.

Canfield, D. E., R. Raiswell, J. T. Westrich, C. M. Reaves, and R. A. Berner. 1986. "The Use of Chromium Reduction in the Analysis of Reduced Inorganic Sulfur in Sediments and Shales." *Chemical Geology* 54: 149–155.

Chang, C., W. Hu, K. Huang, Z. Wang, and X. Zhang. 2023. "Mass Extinction Coincided With Expanded Continental Margin Euxinia During the Cambrian Age 4." *Geophysical Research Letters* 50: e2023GL105560.

Chen, X., S. Li, S. M. Newby, T. W. Lyons, F. Wu, and J. D. Owens. 2022. "Iron and Manganese Shuttle Has no Effect on Sedimentary Thallium and Vanadium Isotope Signatures in Black Sea Sediments." *Geochimica et Cosmochimica Acta* 317: 218–233.

Chen, X., H.-F. Ling, D. Vance, et al. 2015. "Rise to Modern Levels of Ocean Oxygenation Coincided With the Cambrian Radiation of Animals." *Nature Communications* 6: 7142.

Chen, Z., G. Wang, and C. Jin. 2022. "Marine Redox Variation and Hydrographic Restriction in the Early Cambrian Nanhua Basin, South China." *Palaeogeography, Palaeoclimatology, Palaeoecology* 607: 111263.

Cheng, M., C. Li, L. Zhou, et al. 2016. "Marine Mo Biogeochemistry in the Context of Dynamically Euxinic Mid-Depth Waters: A Case Study of the Lower Cambrian Niutitang Shales, South China." *Geochimica et Cosmochimica Acta* 183: 79–93.

Cheng, M., C. Li, L. Zhou, et al. 2017. "Transient Deep-Water Oxygenation in the Early Cambrian Nanhua Basin, South China." *Geochimica et Cosmochimica Acta* 210: 42–58.

Cheng, M., Z. Zhang, C. Jin, et al. 2023. "Salinity Variation and Hydrographic Dynamics in the Early Cambrian Nanhua Basin (South China)." *Science China Earth Sciences* 66: 1268–1278.

Cole, D. B., N. J. Planavsky, M. Longley, et al. 2020. "Uranium Isotope Fractionation in Non-Sulfidic Anoxic Settings and the Global Uranium Isotope Mass Balance." *Global Biogeochemical Cycles* 34: e2020GB006649.

Dahl, T. W., J. N. Connelly, A. Kouchinsky, B. C. Gill, S. F. Månsson, and M. Bizzarro. 2017. "Reorganisation of Earth's Biogeochemical Cycles Briefly Oxygenated the Oceans 520 Myr Ago." *Geochemical Perspectives Letters* 3: 210–220.

Dohrmann, M., and G. Wörheide. 2017. "Dating Early Animal Evolution Using Phylogenomic Data." *Scientific Reports* 7: 3599.

Erwin, D. H., M. Laflamme, S. M. Tweedt, E. A. Sperling, D. Pisani, and K. J. Peterson. 2011. "The Cambrian Conundrum: Early Divergence and Later Ecological Success in the Early History of Animals." *Science* 334: 1091–1097.

Fan, H., X. Fu, R. Yang, et al. 2023. "Hg Isotope Evidence for Oceanic Oxygenation During the Cambrian Explosion." *Geochimica et Cosmochimica Acta* 362: 104–114.

Fan, H., S. G. Nielsen, J. D. Owens, et al. 2020. "Constraining Oceanic Oxygenation During the Shuram Excursion in South China Using Thallium Isotopes." *Geobiology* 18: 348–365.

Feng, L., C. Li, J. Huang, H. Chang, and X. Chu. 2014. "A Sulfate Control on Marine Mid-Depth Euxinia on the Early Cambrian (ca. 529–521Ma) Yangtze Platform, South China." *Precambrian Research* 246: 123–133.

Fu, D., G. Tong, T. Dai, et al. 2019. "The Qingjiang Biota—A Burgess Shale–Type Fossil Lagerstätte From the Early Cambrian of South China." *Science* 363: 1338–1342.

Goldberg, T., G. Gordon, G. Izon, et al. 2013. "Resolution of Inter-Laboratory Discrepancies in Mo Isotope Data: An Intercalibration." *Journal of Analytical Atomic Spectrometry* 28: 724.

Gong, Z., G. Wei, M. Fakhraee, et al. 2023. "Revisiting Marine Redox Conditions During the Ediacaran Shuram Carbon Isotope Excursion." *Geobiology* 21: 407–420.

Han, T., H. Fan, and H. Wen. 2018. "Dwindling Vanadium in Seawater During the Early Cambrian, South China." *Chemical Geology* 492: 20–29.

Hood, A. V. S., N. J. Planavsky, M. W. Wallace, and X. Wang. 2018. "The Effects of Diagenesis on Geochemical Paleoredox Proxies in Sedimentary Carbonates." *Geochimica et Cosmochimica Acta* 232: 265–287.

Jin, C., C. Li, T. J. Algeo, et al. 2016. "A Highly Redox-Heterogeneous Ocean in South China During the Early Cambrian (~529–514 Ma): Implications for Biota-Environment Co-Evolution." *Earth and Planetary Science Letters* 441: 38–51.

Jin, C., C. Li, T. J. Algeo, et al. 2020. "Controls on Organic Matter Accumulation on the Early-Cambrian Western Yangtze Platform, South China." *Marine and Petroleum Geology* 111: 75–87.

Kendall, B., T. W. Dahl, and A. D. Anbar. 2017. "The Stable Isotope Geochemistry of Molybdenum." *Reviews in Mineralogy and Geochemistry* 82: 683–732.

Kendall, B., J. Wang, W. Zheng, et al. 2020. "Inverse Correlation Between the Molybdenum and Uranium Isotope Compositions of Upper Devonian Black Shales Caused by Changes in Local Depositional Conditions Rather Than Global Ocean Redox Variations." *Geochimica et Cosmochimica Acta* 287: 141–164.

Knoll, A. H., and S. B. Carroll. 1999. "Early Animal Evolution: Emerging Views From Comparative Biology and Geology." *Science* 284: 2129–2137.

Lau, K. V., L. G. Hancock, S. Severmann, et al. 2022. "Variable Local Basin Hydrography and Productivity Control the Uranium Isotope Paleoredox Proxy in Anoxic Black Shales." *Geochimica et Cosmochimica Acta* 317: 433–456.

Lau, K. V., S. J. Romaniello, and F. Zhang. 2019. *The Uranium Isotope Paleoredox Proxy*. 1st ed. Cambridge University Press.

Li, C., C. Jin, N. J. Planavsky, et al. 2017. "Coupled Oceanic Oxygenation and Metazoan Diversification During the Early–Middle Cambrian?" *Geology* 45, no. 8: 743–746.

Li, Z., M. Zhang, Z.-Q. Chen, T. J. Algeo, L. Zhao, and F. Zhang. 2021. "Early Cambrian Oceanic Oxygenation and Evolution of Early Animals: A Critical Review From the South China Craton." *Global and Planetary Change* 204: 103561.

Li, Z. X., S. V. Bogdanova, A. S. Collins, et al. 2008. "Assembly, Configuration, and Break-Up History of Rodinia: A Synthesis." *Precambrian Research* 160: 179–210.

Love, G. D., E. Grosjean, C. Stalvies, et al. 2009. "Fossil Steroids Record the Appearance of Demospongiae During the Cryogenian Period." *Nature* 457: 718–721.

Marshall, C. R. 2006. "Explaining the Cambrian "Explosion" of Animals." *Annual Review of Earth and Planetary Sciences* 34: 355–384.

Matthäus, W., D. Nehring, R. Feistel, G. Nausch, V. Mohrholz, and H. Lass. 2008. "The Inflow of Highly Saline Water Into the Baltic Sea." In *State and Evolution of the Baltic Sea, 1952–2005*, edited by R. Feistel, G. Nausch, and N. Wasmund, 265–309. Wiley.

Matthews, A. D., and J. P. Riley. 1969. "The Determination of Thallium in Silicate Rocks, Marine Sediments and Sea Water." *Analytica Chimica Acta* 48: 25–34.

Nägler, T. F., N. Neubert, M. E. Böttcher, O. Dellwig, and B. Schnetger. 2011. "Molybdenum Isotope Fractionation in Pelagic Euxinia: Evidence From the Modern Black and Baltic Seas." *Chemical Geology* 289: 1–11.

Nielsen, S. G., M. Goff, S. P. Hesselbo, H. C. Jenkyns, D. E. LaRowe, and C.-T. A. Lee. 2011. "Thallium Isotopes in Early Diagenetic Pyrite – A Paleoredox Proxy?" *Geochimica et Cosmochimica Acta* 75: 6690–6704.

Nielsen, S. G., F. Klein, T. Kading, J. Blusztajn, and K. Wickham. 2015. "Thallium as a Tracer of Fluid–Rock Interaction in the Shallow Mariana Forearc." *Earth and Planetary Science Letters* 430: 416–426.

Nielsen, S. G., M. Rehkämper, J. Baker, and A. N. Halliday. 2004. "The Precise and Accurate Determination of Thallium Isotope Compositions and Concentrations for Water Samples by MC-ICPMS." *Chemical Geology* 204: 109–124.

Nielsen, S. G., M. Rehkämper, D. Porcelli, et al. 2005. "Thallium Isotope Composition of the Upper Continental Crust and Rivers—An Investigation of the Continental Sources of Dissolved Marine Thallium." *Geochimica et Cosmochimica Acta* 69: 2007–2019.

Nielsen, S. G., L. E. Wasylenki, M. Rehkämper, C. L. Peacock, Z. Xue, and E. M. Moon. 2013. "Towards an Understanding of Thallium Isotope Fractionation During Adsorption to Manganese Oxides." *Geochimica et Cosmochimica Acta* 117: 252–265.

Ostrander, C. M., C. J. Bjerrum, A. C. Ahm, et al. 2023. "Widespread Seafloor Anoxia During Generation of the Ediacaran Shuram Carbon Isotope Excursion." *Geobiology* 21: 556–570.

Ostrander, C. M., J. D. Owens, and S. G. Nielsen. 2017. "Constraining the Rate of Oceanic Deoxygenation Leading Up to a Cretaceous Oceanic Anoxic Event (OAE-2: ~94 Ma)." *Science Advances* 3: e1701020.

Ostrander, C. M., J. D. Owens, S. G. Nielsen, et al. 2020. "Thallium Isotope Ratios in Shales From South China and Northwestern Canada Suggest Widespread O2 Accumulation in Marine Bottom Waters Was an Uncommon Occurrence During the Ediacaran Period." *Chemical Geology* 557: 119856.

Ostrander, C. M., Y. Shu, S. G. Nielsen, et al. 2024. "Anthropogenic Forcing of the Baltic Sea Thallium Cycle." *Environmental Science & Technology* 58: 8510–8517.

Owens, J. D., S. G. Nielsen, T. J. Horner, C. M. Ostrander, and L. C. Peterson. 2017. "Thallium-Isotopic Compositions of Euxinic Sediments as a Proxy for Global Manganese-Oxide Burial." *Geochimica et Cosmochimica Acta* 213: 291–307.

Payne, J. L., A. G. Boyer, J. H. Brown, et al. 2009. "Two-Phase Increase in the Maximum Size of Life Over 3.5 Billion Years Reflects Biological Innovation and Environmental Opportunity." *Proceedings of the National Academy of Sciences* 106: 24–27.

Peacock, C. L., and E. M. Moon. 2012. "Oxidative Scavenging of Thallium by Birnessite: Explanation for Thallium Enrichment and Stable Isotope Fractionation in Marine Ferromanganese Precipitates." *Geochimica et Cosmochimica Acta* 84: 297–313.

Phillips, R. F., Y. Wang, F. Klein, et al. 2023. "The Role of Manganese Oxide Mineralogy in Thallium Isotopic Fractionation Upon Sorption." *Geochimica et Cosmochimica Acta* 356: 83–92.

Poulton, S. W., and D. E. Canfield. 2005. "Development of a Sequential Extraction Procedure for Iron: Implications for Iron Partitioning in Continentally Derived Particulates." *Chemical Geology* 214: 209–221.

Poulton, S. W., and D. E. Canfield. 2011. "Ferruginous Conditions: A Dominant Feature of the Ocean Through Earth's History." *Elements* 7: 107–112.

Qin, Z., D. Xu, B. Kendall, et al. 2022. "Molybdenum Isotope-Based Redox Deviation Driven by Continental Margin Euxinia During the Early Cambrian." *Geochimica et Cosmochimica Acta* 325: 152–169.

Rehkämper, M., M. Frank, J. R. Hein, et al. 2002. "Thallium Isotope Variations in Seawater and Hydrogenetic, Diagenetic, and Hydrothermal Ferromanganese Deposits." *Earth and Planetary Science Letters* 197: 65–81.

Rehkämper, M., and S. G. Nielsen. 2004. "The Mass Balance of Dissolved Thallium in the Oceans." *Marine Chemistry* 85: 125–139.

Rhoads, D. C., and J. W. Morse. 1971. "Evolutionary and Ecological Significance of Oxygen-Deficient Marine Basins." *Lethaia* 4: 413–428.

Rudnick, R. L., and S. Gao. 2014. "Composition of the Continental Crust." In *Treatise on Geochemistry*, 1–51. Elsevier.

Scholz, F., J. McManus, and S. Sommer. 2013. "The Manganese and Iron Shuttle in a Modern Euxinic Basin and Implications for Molybdenum Cycling at Euxinic Ocean Margins." *Chemical Geology* 355: 56–68.

Smith, E. F., F. A. Macdonald, T. A. Petach, U. Bold, and D. P. Schrag. 2016. "Integrated Stratigraphic, Geochemical, and Paleontological Late Ediacaran to Early Cambrian Records From Southwestern Mongolia." *Geological Society of America Bulletin* 128: 442–468.

Sperling, E. A., C. A. Frieder, A. V. Raman, P. R. Girguis, L. A. Levin, and A. H. Knoll. 2013. "Oxygen, Ecology, and the Cambrian Radiation of Animals." *Proceedings of the National Academy of Sciences* 110: 13446–13451.

Sperling, E. A., A. H. Knoll, and P. R. Girguis. 2015. "The Ecological Physiology of Earth's Second Oxygen Revolution." *Annual Review of Ecology, Evolution, and Systematics* 46: 215–235.

Sperling, E. A., C. J. Wolock, A. S. Morgan, et al. 2015. "Statistical Analysis of Iron Geochemical Data Suggests Limited Late Proterozoic Oxygenation." *Nature* 523: 451–454.

Steiner, M., G. Li, Y. Qian, M. Zhu, and B.-D. Erdtmann. 2007. "Neoproterozoic to Early Cambrian Small Shelly Fossil Assemblages and a Revised Biostratigraphic Correlation of the Yangtze Platform (China)." *Palaeogeography, Palaeoclimatology, Palaeoecology* 254: 67–99.

Stockey, R. G., D. B. Cole, U. C. Farrell, et al. 2024. "Sustained Increases in Atmospheric Oxygen and Marine Productivity in the Neoproterozoic and Palaeozoic Eras." *Nature Geoscience* 17: 667–674.

Them, T. R., B. C. Gill, A. H. Caruthers, et al. 2018. "Thallium Isotopes Reveal Protracted Anoxia During the Toarcian (Early Jurassic) Associated With Volcanism, Carbon Burial, and Mass Extinction." *Proceedings of the National Academy of Sciences* 115: 6596–6601.

Tribovillard, N., T. J. Algeo, F. Baudin, and A. Riboulleau. 2012. "Analysis of Marine Environmental Conditions Based Onmolybdenum–Uranium Covariation—Applications to Mesozoic Paleoceanography." *Chemical Geology* 324–325: 46–58.

Van Helmond, N. A. G. M., T. Jilbert, and C. P. Slomp. 2018. "Hypoxia in the Holocene Baltic Sea: Comparing Modern Versus Past Intervals Using Sedimentary Trace Metals." *Chemical Geology* 493: 478–490.

Wang, J., and Z.-X. Li. 2003. "History of Neoproterozoic Rift Basins in South China: Implications for Rodinia Break-Up." *Precambrian Research* 122: 141–158.

Wang, X., X. Shi, X. Zhao, and D. Tang. 2015. "Increase of Seawater Mo Inventory and Ocean Oxygenation During the Early Cambrian." *Palaeogeography, Palaeoclimatology, Palaeoecology* 440: 621–631.

Wang, Y., W. Lu, K. M. Costa, and S. G. Nielsen. 2022. "Beyond Anoxia: Exploring Sedimentary Thallium Isotopes in Paleo-Redox Reconstructions From a New Core Top Collection." *Geochimica et Cosmochimica Acta* 333: 347–361.

Wei, G.-Y., N. J. Planavsky, T. He, et al. 2021. "Global Marine Redox Evolution From the Late Neoproterozoic to the Early Paleozoic Constrained by the Integration of Mo and U Isotope Records." *Earth-Science Reviews* 214: 103506.

Wei, G.-Y., N. J. Planavsky, L. G. Tarhan, et al. 2018. "Marine Redox Fluctuation as a Potential Trigger for the Cambrian Explosion." *Geology* 46: 587–590.

Wei, G.-Y., N. J. Planavsky, L. G. Tarhan, et al. 2020. "Highly Dynamic Marine Redox State Through the Cambrian Explosion Highlighted by Authigenic δ238U Records." *Earth and Planetary Science Letters* 544: 116361.

Wen, H., H. Fan, Y. Zhang, C. Cloquet, and J. Carignan. 2015. "Reconstruction of Early Cambrian Ocean Chemistry From Mo Isotopes." *Geochimica et Cosmochimica Acta* 164: 1–16.

Wood, R., A. G. Liu, F. Bowyer, et al. 2019. "Integrated Records of Environmental Change and Evolution Challenge the Cambrian Explosion." *Nature Ecology & Evolution* 3: 528–538.

Xu, L., B. Lehmann, J. Mao, et al. 2012. "Mo Isotope and Trace Element Patterns of Lower Cambrian Black Shales in South China: Multi-Proxy Constraints on the Paleoenvironment." *Chemical Geology* 318–319: 45–59.

Yang, C., X.-H. Li, M. Zhu, D. J. Condon, and J. Chen. 2018. "Geochronological Constraint on the Cambrian Chengjiang Biota, South China." *Journal of the Geological Society* 175: 659–666.

Zhang, H., H. Fan, F. Zhang, and H. Wen. 2023. "Paleosalinity of the Nanhua Basin (South China) During the Cambrian Explosion." *Palaeogeography, Palaeoclimatology, Palaeoecology* 627: 111716.

Supporting Information

Additional supporting information can be found online in the Supporting Information section. **Table S1:** Geochemical data for the Qingjiang and Weng'an sections.